https://doi.org/10.5194/npg-2020-45
Preprint. Discussion started: 9 March 2021
© Author(s) 2021. CC BY 4.0 License.

Nonlinear Processes in Geophysics
Discussions
Open Access

Analytical Solution for the Influence of Irregular Shape Loads Near the Borehole Strain Observation

Wei YAN *(1),(2) , Zirui LI (3)

(1) Institute of Geology, China Earthquake Administration, Beijing 100026, China
(2) China Earthquake Networks Center, Beijing 100045, China
(3) Ningxia Seismological Brueau, Yinchuan 750001, China

Abstract

Based on the analytic displacement solution caused by the punctate load model, we derived the calculation formulas of peripheral strain Field. This method can provide a theoretical basis for the quantitative calculation of the load influence of borehole strain observation. On this basis, using the superposition principle, we present a method for calculating the strain effect of two-dimensional and three-dimensional irregular shape loads. The results show that: (1) To solve the problem of two-dimensional irregular shape load model, we can calculate it by vector superposition after load scattering. (2) To solve the problem of three-dimensional irregular shape load model, we can use the two-dimensional irregular shape load method to calculate with assigning different weights to the scattered points after the load scattering. (3) There are obvious convergence processes in the vector superposition process after scattering of two-dimensional and three-dimensional irregular loads, which shows the correctness and feasibility of the calculation method. (4) The calculation method introduced in this paper can provide a research basis for quantitative analysis of influence of disturbance of peripheral load in borehole strain observation.

Keywords

Borehole strain observation; punctate load model; Irregular shape load; Superposition principle; Scattering

1 Introduction

Borehole strain observation is one of the most important observation tools to capturing

https://doi.org/10.5194/npg-2020-45
Preprint. Discussion started: 9 March 2021
© Author(s) 2021. CC BY 4.0 License.
Nonlinear Processes in Geophysics
Discussions

information of crustal stress change before an earthquake. Borehole strain observation has advantages over other precursor observation methods. A borehole strain observation network has been set up in the PBO project in the United States (David et al., 2002). The advantages of borehole strain observation mainly lie in its high accuracy and data can be self-checked (Chi,1993; Ouyang et al., 2009; Li et al., 2004). Since 1990, China Earthquake Precursor Observation System has built more than 1000 strain observation points, which provides a large amount of data support for crustal deformation monitoring. Many researchers have discussed the deformation characteristics of deformation before earthquakes (Zhang et al., 2007, 2009; Qiu et al., 2010; Niu et al., 2009, 2012, 2013). However, economic constructions around observation stations has caused great interference, such as building buildings, storing water in reservoirs, accumulating rocks and so on.

The theoretical analysis of the influence of load on the observation of surrounding deformation has research significance in the observation of earthquake precursors or the monitoring of foundation settlement (Zhang, 2013; Huang, 2002; Yang et al., 2002). Because the actual loads are mostly irregular shapes, many researchers use numerical analysis to discuss the displacement and strain solutions around the loads (Wang et al., 2000, 2002; Du et al., 2004). Some other researchers have obtained the approximate analytical solution of this problem by simplifying the model into a punctate load model (Hu et al., 2002; Qiu, 2004; Luo et al., 2008; Li et al., 2007). Since the simplified model can only provide an approximate solution, this paper mainly focuses on the exact solution of strain field for irregular shape loads. In this paper, the strain symbols obey the elasticity rules, which means the tension is positive and the pressure is negative.

2 Strain Analytical Solution of Punctate Load Model and its Distribution

When a vertical concentrated force P forced on the surface of a homogeneous, isotropic semi-infinite elastic body (Fig. 1).

https://doi.org/10.5194/npg-2020-45
Preprint. Discussion started: 9 March 2021
© Author(s) 2021. CC BY 4.0 License.
Nonlinear Processes in Geophysics
Discussions
Open Access

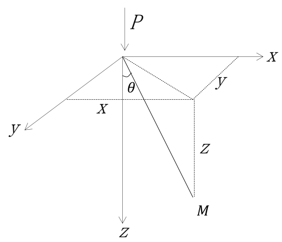

Fig.1 The sketch map of punctate load model's coordination system

The vertical normal stress and horizontal displacement at any point $M(x,y,z)$ can be calculated by the Boussinesq solution (Boussinesq, 1885). The x-direction linear stress σ_x, y-direction linear stress σ_y, x-direction displacement u and y-direction horizontal displacement v of point $M(x,y,z)$ can be expressed as follows:

$$\sigma_x = \frac{3P}{2\pi}\left[\frac{x^2 z}{R^5} + \frac{1-2\mu}{3}\left(\frac{R^2 - Rz - z^2}{R^3(R+z)}\right) - \frac{x^2(2R+z)}{R^3(R+z)^2}\right] \tag{1}$$

$$\sigma_y = \frac{3P}{2\pi}\left[\frac{y^2 z}{R^5} + \frac{1-2\mu}{3}\left(\frac{R^2 - Rz - z^2}{R^3(R+z)}\right) - \frac{y^2(2R+z)}{R^3(R+z)^2}\right] \tag{2}$$

$$u = \frac{P(1+\mu)}{2\pi E}\left[\frac{xz}{R^3} - (1-2\mu)\frac{x}{R(R+z)}\right] \tag{3}$$

$$v = \frac{P(1+\mu)}{2\pi E}\left[\frac{yz}{R^3} - (1-2\mu)\frac{y}{R(R+z)}\right] \tag{4}$$

Among them, R is the distance from point M to point P, E is Young's modulus and μ is Poisson's ratio, and the relationship between R and the coordination is:

$$R = \sqrt{x^2 + y^2 + z^2} \tag{5}$$

According to the relationship between displacement and linear strain, the linear strain in the direction of x and y can be calculated by the first derivative of displacement u and v respectively.

$$\varepsilon_x = \frac{\partial u}{\partial x} = \frac{P(1+\mu)}{2\pi E}\left[\frac{R^2 z - 3x^2 z}{R^5} - (1-2\mu)\frac{R^3 + R^2 z - x^2(2R+z)}{R(R^2+Rz)^2}\right] \tag{6}$$

$$\varepsilon_y = \frac{\partial v}{\partial y} = \frac{P(1+\mu)}{2\pi E}\left[\frac{R^2 z - 3y^2 z}{R^5} - (1-2\mu)\frac{R^3 + R^2 z - y^2(2R+z)}{R(R^2+Rz)^2}\right] \tag{7}$$

According to the relationship between area strain and two orthogonal linear strains, area strain ε_s can be expressed as:

$$\varepsilon_s = \varepsilon_x + \varepsilon_y \tag{8}$$

https://doi.org/10.5194/npg-2020-45
Preprint. Discussion started: 9 March 2021
© Author(s) 2021. CC BY 4.0 License.
Nonlinear Processes in Geophysics
Open Access
Discussions
EGU

Formulas 6, 7 and 8 are analytical solutions to the strain field around a punctate load model, we can use them to solve the strain parameters in any point around the location of force *P*. Taking sand-rock as an example, Young's modulus E=4×10^{7}Pa, Poisson's ratio μ=0.25 and load force P=2×10^{4}N, the spatial distribution of strain field of horizontal slices at depth of 0.1m can be calculated. The results are shown in figure 2.

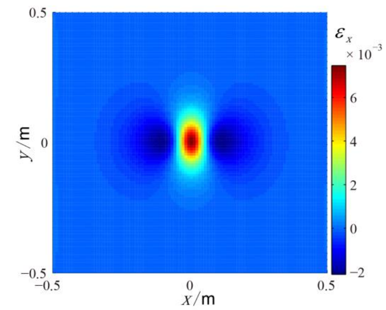

(a)

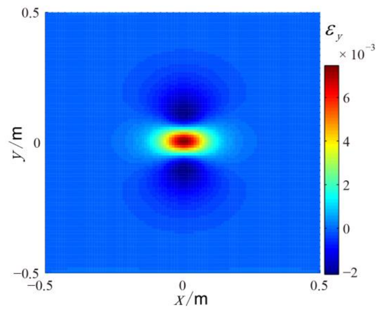

(b)

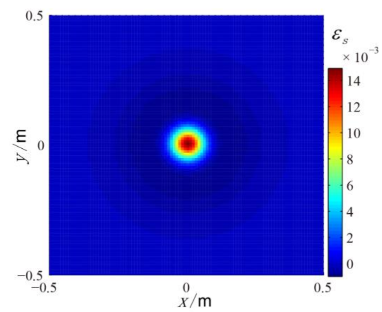

(c)

Fig.2 The strain field distribution around the punctate load model of horizontal slices at depth of 0.1m
(a)The linear strain ε_x; (b)The linear strain ε_y; (c)The area strain ε_s

From Figure 2, it can be seen that the linear strain distribution presents a tense strain (positive value) in a small area near the load center, and a compressive strain (negative value) far from the load center (Fig. 2ab). The area strain distribution presents expansion strain phenomenon near the load center, and compression strain far from the load center (Fig. 2c).

3 Strain Analytical Solution of Irregular Load Model and its Distribution

Because the point load is an ideal model and the shape of actual load is irregular, it is necessary to discuss the calculation method of irregular shape load model when analyzing

https://doi.org/10.5194/npg-2020-45
Preprint. Discussion started: 9 March 2021
© Author(s) 2021. CC BY 4.0 License.
Nonlinear Processes in Geophysics
Open Access
Discussions
EGU

practical problems. In this paper, irregular loads are divided into two-dimensional irregular and three-dimensional irregular shape loads.

3.1 Strain Analytical Solution of Irregular Load Model in two-dimensional and its Distribution

According to the principle of superposition, for the two-dimensional irregular shape load model, the total force P can be scattered as P_i. The scattered strain analytical solution of irregular load model in two-dimensional can be calculated using the formula (6), (7). Assuming that the number of scattered grids is n, the relationship between each variables is as follows:

$$P_i = \frac{P}{n} \tag{9}$$

$$\varepsilon_x = \sum \varepsilon_{xi} \tag{10}$$

$$\varepsilon_y = \sum \varepsilon_{yi} \tag{11}$$

The scattering process is shown in Figure 3. In practical calculation, on the basis of gridding, the scattered linear strain ε_{xi}, ε_{yi} of M point can be calculated by using formulas (6) and (7), respectively, and then the vector superposition strain ε_x, ε_y can be calculated by using formula (10) and (11).

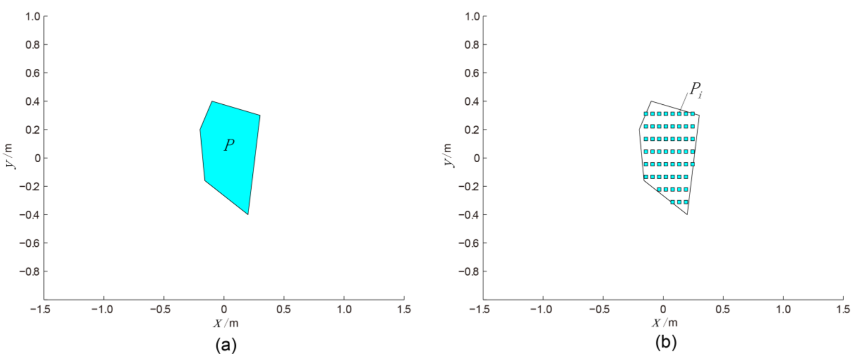

Fig.3 The scattering process diagram of two dimensional irregular load model

Because of the scattered processing, it is necessary to verify the convergence characteristics of the calculated results with the change of grid count n. Figure 6 shows the relationship between the horizontal displacement & linear strain at point M(1.5m, -1.5m, -0.2m) and the number of grids n under the conditions of Young's modulus E = 4×10^7 Pa, Poisson's ratio μ = 0.25 and total

https://doi.org/10.5194/npg-2020-45
Preprint. Discussion started: 9 March 2021
© Author(s) 2021. CC BY 4.0 License.

load force $P = 2\times10^4$ N.

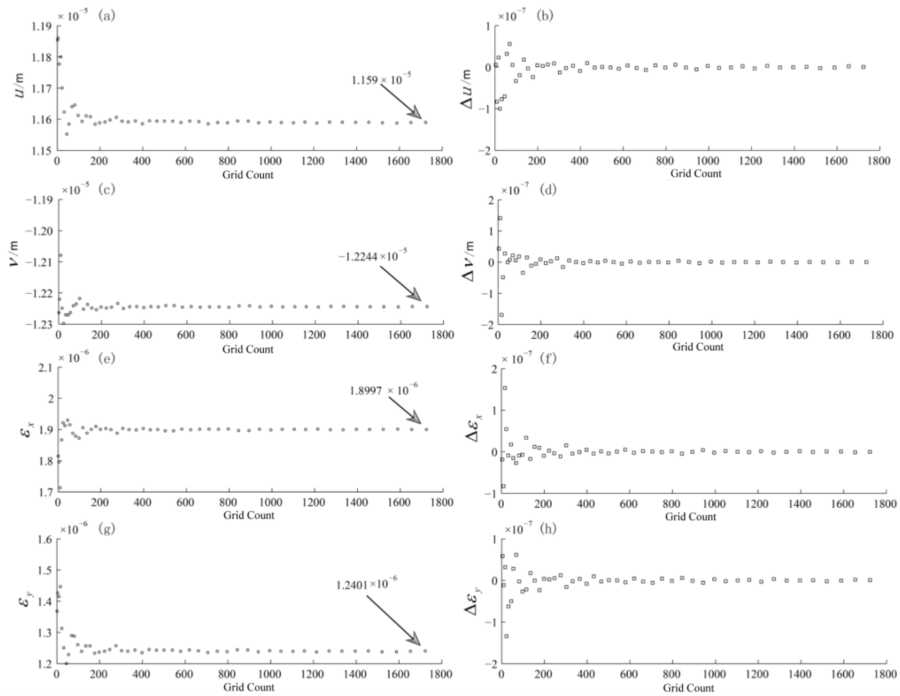

Fig.4 The relationship between the horizontal displacement & linear strain and the change of grid count *n* in the point of M(1.5m, -1.5m, -0.2m) using the model of two dimensional irregular load

(a) the relationship between displacement *u* and grid count *n*; (c) the relationship between displacement *v* and grid count *n*; (e) the relationship between linear strain ε_x and grid count *n*; (g) the relationship between linear strain ε_y and grid count *n*; (b),(d),(f),(h) are the first-order differences of data of (a),(c),(e),(g) respectively.

It can be seen from figure 4 that with the increase of the grid count *n*, the displacements *u* and *v* converge to 1.159×10^{-5} m and -1.2244×10^{-5} m respectively (Fig.6a,c). The linear strains ε_x and ε_y converge to 1.8997×10^{-6} and 1.2401×10^{-6} respectively (Fig.6e,g). The first-order differences of above parameters are all converge to 0, which means that it is correct and feasible to use scattering method to calculate two-dimensional irregular shape load model.

For the two-dimensional irregular shape load shown in figure 3, taking sand-rock as an example (Young's modulus E = 10 Pa, Poisson's ratio μ = 0.25, load force P = 10 N), the spatial distribution of horizontal strain field at 0.2m depth is shown in figure 5.

https://doi.org/10.5194/npg-2020-45
Preprint. Discussion started: 9 March 2021
© Author(s) 2021. CC BY 4.0 License.

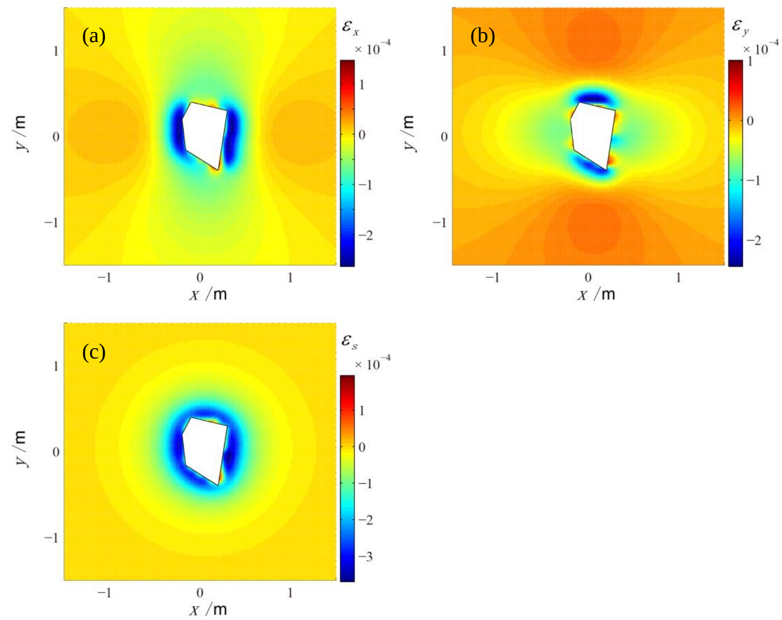

Fig.5 The strain field displacement around the 2D irregular load model in the depth of 0.2m

(a)The linear strain ε_x ; (b)The linear strain ε_y ; (c)The area strain ε_s; the white polygon represents the shape of irregular load

As can be seen from figure 5, the strain field around two-dimensional irregular loads is compressive (negative value). The spatial distribution of strain field has a certain spatial correlation (Fig.5a,b). In the near field, the area strain ε_s is related to the shape of the load. In the far field, the strain field is nearly circular, which shows that the irregular load can be simplified to a punctate load model in the far field. In other words, when irregular load is close to the borehole strain instrument, we can not simplify the whole load to a punctate load model to calculate.

3.2 Strain Analytical Solution of Irregular Load Model in Three-dimensional irregular shape and its Distribution

The method to solve the influence of three-dimensional irregular load is basically similar with that of two-dimensional load model. It is also based on scattering irregular shape load (Fig.6). The differences are as follows: (1) For three-dimensional irregular shape loads with uniform density, the height of scattered points H_i are redistributed as weight to the total load P (Fig. 6); (2) For three-dimensional irregular shape loads with uneven density, the scattered height H_i and density ρ_i can be used as weight to redistribute the loads.

https://doi.org/10.5194/npg-2020-45
Preprint. Discussion started: 9 March 2021
© Author(s) 2021. CC BY 4.0 License.

$$P_i = \frac{P}{n} \cdot \frac{H_i \rho_i}{\sum H_i \rho_i} \tag{12}$$

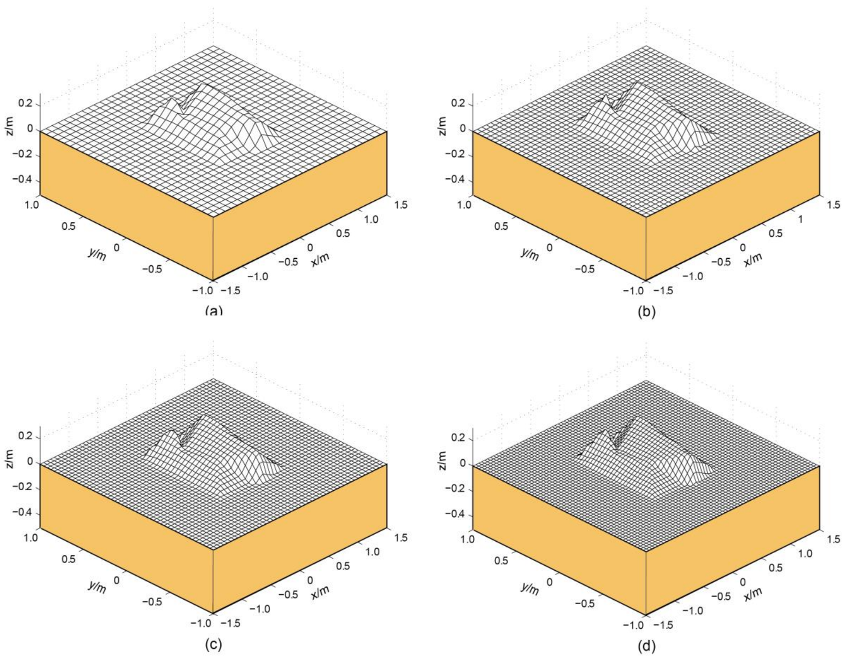

Fig.6 The scatter process diagram of three dimensional irregular load model in different grid count *n*

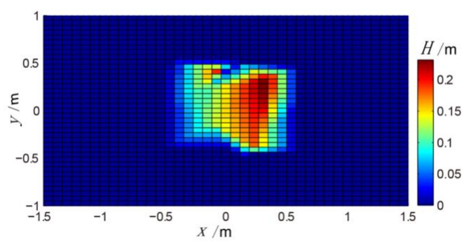

Fig.7 The height distribution of three dimensional irregular load model

Because there are no significant differences between the uneven density and uniform density in the process of processing, in order to clearly explain the method of load modeling, this paper mainly focuses on discussing the method of establishing the three-dimensional load model with uniform density. Similar to the two-dimensional irregular shape load model, due to the scattering process, it is necessary to verify the convergence characteristics of the calculated results with the count of grids *n*. The calculation results are shown in figure 8.

https://doi.org/10.5194/npg-2020-45
Preprint. Discussion started: 9 March 2021
© Author(s) 2021. CC BY 4.0 License.

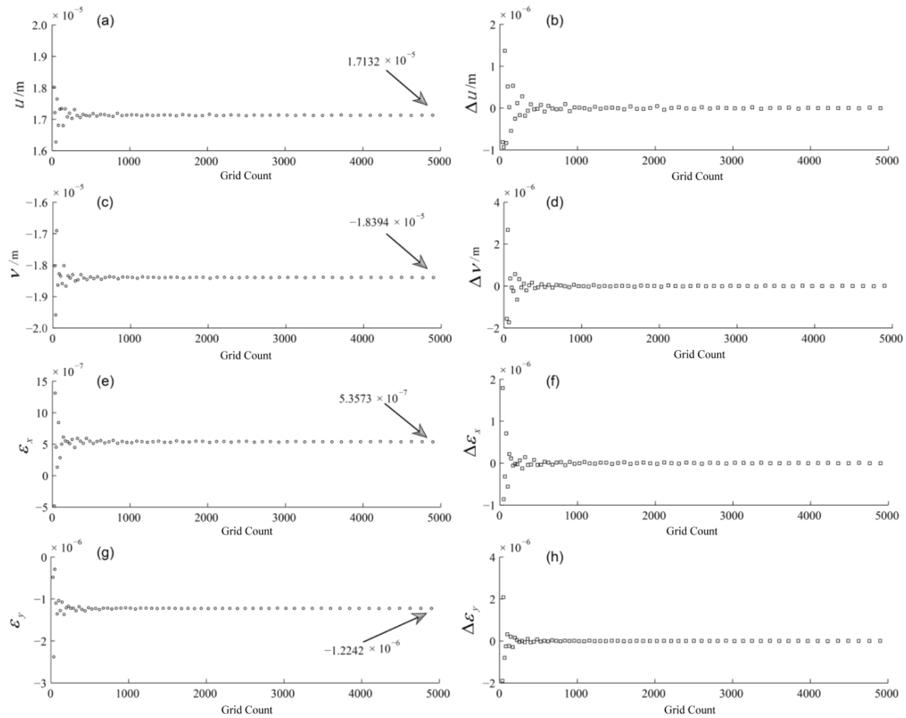

Fig.8 The relationship between the horizontal displacement & linear strain and the change of grid count *n* in the point of M(1.5m, -1.5m, -0.1m) using the model of three dimensional irregular load

(a) the relationship between displacement *u* and grid count *n*; (c) the relationship between displacement *v* and grid count *n*; (e) the relationship between linear strain ε_x and grid count *n*; (g) the relationship between linear strain ε_y and grid count *n*; (b),(d),(f),(h) are the first-order differences of data of (a),(c),(e),(g) respectively.

Figure 8 shows the relationship between the horizontal displacement and strain at point M (1.5m, -1.5m, -0.1m) and the number of grids *n* under the conditions of Young's modulus E = 4×10^7 Pa, Poisson's ratio u=0.25 and total load $P = 2\times10^4$ N using the model of three dimensional irregular load. It can be seen that with the increase of the number of grids *n*, the displacements *u* and *v* converge to $1.7132\times10\text{-}^5$m and -1.8394×10^{-5}m respectively (Fig. 6a,c). The linear strains ε_x and ε_y converges to 5.3573×10^{-7} and -1.2242×10^{-7} respectively (Fig. 6e,g). The first-order differences of above parameters are all converge to 0, which means that it is correct and feasible to use scattering method to calculate three-dimensional irregular shape load model.

For the three-dimensional irregular shape load shown in Figure 6, taking sand-rock as an example, the spatial distribution of horizontal strain field at 0.2m depth is shown in Figure 9.

https://doi.org/10.5194/npg-2020-45
Preprint. Discussion started: 9 March 2021
© Author(s) 2021. CC BY 4.0 License.

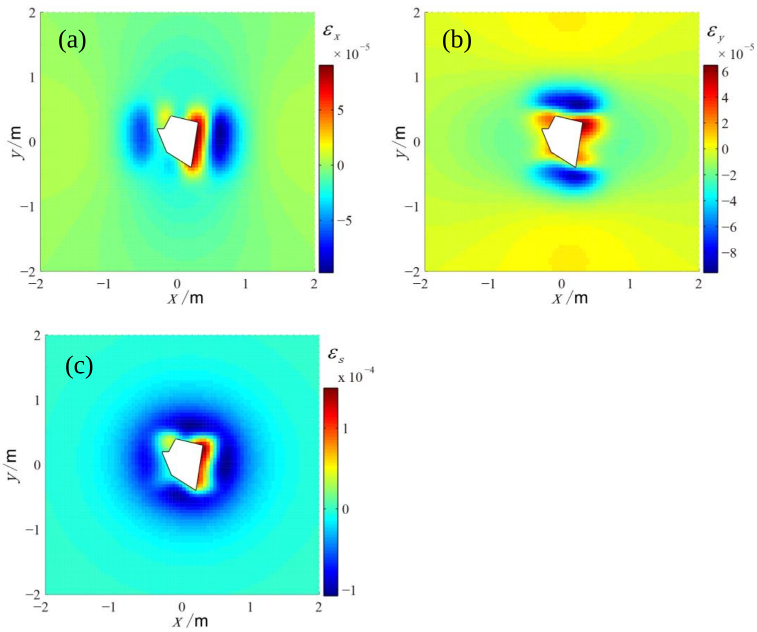

Fig.9 The strain field displacement around the 3D irregular load model in the depth of 0.2m

(a)The linear strain ε_x ; (b)The linear strain ε_y ; (c)The area strain ε_s; the white polygon represents the shape of irregular load

It can be seen from figure 9 that the spatial distribution of the strain field in the three-dimensional irregular load model is more complex than that in the two-dimensional irregular load model. This inhomogeneity is related not only to the irregular distribution of the plane projection shape of the irregular load, but also to the non-uniformity of its elevation distribution.

4 Conclusions

We can simplify an irregular shape load to a punctate load on the hypothesis that the distance is long enough, which can not solve the problem of the influence of short distance load on borehole strain observation. In this paper, the quantitative calculation methods and examples of analytical solutions of borehole strain observation caused by punctate load, two-dimensional and three-dimensional irregular load are given. The development of this work can provide a theoretical analysis basis for the influence of peripheral load on borehole strain observation.

Through the above calculation and analysis, the results show that:

(1)The influence of punctate load on borehole strain observation can be calculated by the

https://doi.org/10.5194/npg-2020-45
Preprint. Discussion started: 9 March 2021
© Author(s) 2021. CC BY 4.0 License.

formulas (6) and (7). The characteristics of strain field around punctate load can be described as: Tension strain occurs in a small area of the compressive load center, compression strain occurs far from the area, and the strain value decreases rapidly with the increase of distance.

(2)The influence of two-dimensional irregular load on borehole strain observation can be firstly scattered, then the strain vector of each scatter point on the borehole probe can be obtained by using the punctate load model, and finally the influence of the irregular load can be obtained by vector superposition.

(3)The calculation method of stress field of three-dimensional irregular load is basically the same as that of two-dimensional irregular load. The difference is related not only to the irregular distribution of the plane projection shape of the irregular load, but also to the non-uniformity of its elevation distribution in the three-dimensional irregular load model.

Reference

1. David S., Willam P., Mark Z., 2002, EarthScope: Acquisition, Construction, Integration and Facility Management. A Collaborative Proposal to NSF
2. Chi Shunliang, 1993. Test and observation results of a shallow borehole YRY-2 borehole strain gauge at 8 stations in North China. Journal of Seismology, 15(2), 224-230
3. Ouyang Zuxi, Zhang Jun, Chen Zheng, etc., 2009, New Progress of Comprehensive Observation Technology for Crustal Deformation Deep Wells, International Earthquake Dynamics, 11,1-13
4. Li Hailiang, Ma Hongjun, Zhang Jun, 2004, FZY-1 Component Borehole Strain Meter Design, Seismic and Geomagnetic Observation and Research, 25 (1), 69-77
5. Zhang Jing, Chen Ronghua and Yang Linzhang, 2006, Identification and Mechanism of Deformation Tidal Anomalies before Strong Earthquakes, Journal of Seismology, 28 (2), 150-157
6. Zhang Jing, Jiang Xiesen and Fang Ying, 2007, Wen'an Earthquake and Digital Strain Data Analysis in Capital Circle Area, Earthquake, 27(1), 39-46
7. Zhang Jing, Jiang Xiesen, Fang Ying et al. 2009. Quantitative analysis of surface tectonic deformation by comprehensive deformation observation. Earthquakes, 29(2), 32-39
8. Qiu Zehua, Zhang Baohong, Chi Shunliang, etc., anomalous strain changes observed at Guzan station before the Wenchuan earthquake in 2010, Chinese Science (Series D), 40 (8), 1031-1039
9. Qiu Zehua, 2014, Several Issues Concerning Monitoring Strong Earthquake Precursors with Dense Borehole Strain Network, Journal of Seismology, 36(4), 738-749
10. Niu Anfu, Zhang Lingkong, Yan Wei, et al. 2009. Study on the characteristics of topographic deformation in the north-central segment of the North-South seismic belt before the

© Author(s) 2021. CC BY 4.0 License.

Wenchuan earthquake. Earthquakes, 29 (1), 100-107

11. Niu Anfu, Zhang Lingkong, Yan Wei, etc. Analysis of Short-term Precursor Phenomena of Topographic Deformation near the Focus of Wenchuan Earthquake in 2012, Earthquake, 32(2), 52-63
12. Niu Anfu, Gu Guohua, Cao Jingpeng, et al. Spatial-temporal evolution characteristics of far-field and near-field deformation before Lushan MS7.0 earthquake, 2013. Journal of Seismology, 35 (5), 670-680
13. Zhang Huilan, 2013, Research on the Impact of Building Load Location and Size on Surface and Tunnel, Transportation and Architecture Science, 5 (10), 149-151
14. Huang Qingheng, 2005, Study on Load Transfer Factor of Thick Sandy Soil on Key Roof Layers, Journal of Geotechnical Engineering, 27(6), 672-676
15. Yang Guochun, Wu Yinzhu, Yu Bo et al., 2002, Research on Deep Plate Load Test of High-rise Buildings, Geology and Exploration, 38 (4), 90-93
16. Wang H., 2000, Surface vertical displacements and level plane changes in the front reservoir area caused by filling the Three Gorges Reservoir, Journal of Geophysical Research, 105(B6), 13211~13220
17. Wang H., Hsu H., Zhu Y., 2002, Prediction of surface horizontal displacements, and gravity and tilt changes caused by filling the Three Gorges Reservoir, Journal of Geodesy, 76(2), 105~114
18. Du Ruilin, Qiao Xuejun, Wang Qi, 2004, Crustal Deformation-GPS Observation Research on Water Storage Load of the Three Gorges Reservoir of the Yangtze River, Advances in Natural Science, 14(9), 1006-1011
19. 19. Hu Weijian, Zhang Junshan, Xie Zhi, Wang Zhimin, Li An-yin, Feng Jianmin, Liu Lijun. Experiments and mechanical analysis of the effect of load on borehole strain measurement [J].Earthquake 2002.doi: 10.3969/j.issn.1000-3274.2002.03.016, 22(3), 95-104
20. 20. Qiu Zehua, 2004, Theoretical Analysis of Minimum "Quiet" Distance from Borehole Strain Observation Point to Surface Load Disturbance Source, Journal of Rock Mechanics and Engineering, 23 (23), 4063-4067
21. Luo Mingjin, Chi Shunliang and Ma Hongjun, 2008. Absolute stress measurement and borehole strain measurement. Beijing: Seismological Press, 170-177
22. Li Zuning, Wu Shaozu, Chen Guang et al. 2007. Using point load superposition method to study short-leveling anomaly data across fault in Tianma, earthquake research, 30 (1), 35-38
23. Boussinesq, J. , 1885, Application des Potentiels a L'etude de l'equilibre et due Mouvement des Solides Elastique. Gauthier Villars, Paris

Acknowledgement

This work has been consulted and discussed with professor Niu Anfu of China Earthquake Network Center and professor Zhang Jing of Institute of Seismic Prediction, China Earthquake Administration. This paper is supported by the Major State Basic Research Development Program of China(Grant No.2017YFC1500502-05) and the Project supported by the National Natural

https://doi.org/10.5194/npg-2020-45
Preprint. Discussion started: 9 March 2021
© Author(s) 2021. CC BY 4.0 License.

Science Foundation of China(Grant No.11672258).

Author Contributions

Wei YAN designed the algorithm and calculated the cases, Telephone Number: (+86)10-59959314, Email: ywpro@163.com; Zirui LI checked the calculation results.

Additional Information

Competing interests: The authors declare no competing interests.